Kinetics of Electron Transfer between Cytochromes *c'* and the Semiquinones of Free Flavin and Clostridial Flavodoxin†

T. E. Meyer,‡ G. Cheddar,‡ R. G. Bartsch,§ E. D. Getzoff,‖ M. A. Cusanovich,*,‡ and G. Tollin‡

Department of Biochemistry, University of Arizona, Tucson, Arizona 85721, Department of Chemistry, University of California at San Diego, La Jolla, California 92093, and Department of Molecular Biology, Research Institute of Scripps Clinic, La Jolla, California 92037

Received August 14, 1985

ABSTRACT: Rate constants have been measured for the reactions of a series of high-spin cytochromes *c'* and their low-spin homologues (cytochromes *c*-554 and *c*-556) with the semiquinones of free flavins and flavodoxin. These cytochromes are approximately 3 times more reactive with lumiflavin and riboflavin semiquinones than are the *c*-type cytochromes that are homologous to mitochondrial cytochrome *c*. We attribute this to the greater solvent exposure of the heme in the *c'*-type cytochromes. In marked contrast, the cytochromes *c'* are 3 orders of magnitude less reactive with flavodoxin semiquinone than are the *c*-type cytochromes. We interpret this result to be a consequence of the location of the exposed heme in cytochrome *c'* at the bottom of a deep groove in the surface of the protein, which is approximately 10–15 Å deep and equally as wide. While free flavins are small enough to enter the groove, the flavin mononucleotide (FMN) prosthetic group of flavodoxin is apparently prevented by steric constraints from approaching the heme more closely than approximately 10 Å without dynamic structural rearrangements. Most cytochromes *c'* are dimeric, but a few are monomeric. The three-dimensional structure of the *Rhodospirillum molischianum* cytochrome *c'* dimer suggests that the heme should be more exposed in the monomer than in the dimer, but no relationship is observed between intrinsic reactivity toward free flavin semiquinones and the aggregation state of the protein. Likewise, there is no evidence that the spin state or ligand field of the iron has any effect on intrinsic reactivity. However, three cytochromes have anomalously low reactivities. Presumably, these proteins have somewhat different surface topography near the heme such that access is more restricted. Electrostatic interactions at the electron-transfer site were investigated with FMN semiquinone, which has a net negative charge. Although there are two conserved basic residues near the heme in the cytochromes *c'*, some proteins showed a negatively charged interaction site with FMN. Furthermore, the magnitude of the effects did not correlate with net protein charge. Computer modeling of the electrostatic potential at the molecular surface of *R. molischianum* cytochrome *c'* shows that, although complex, the ionic strength effects on kinetics can be rationalized in terms of basic residues near the heme. Amino acid substitutions in other species appear to be consistent with the involvement of these residues in the electrostatic interaction. The results are consistent with those obtained with *c*-type cytochromes and high redox potential ferredoxins (HiPIP's) and demonstrate that charged amino acid residues nearest the site of electron transfer dominate electrostatic interactions, but more distant residues (or, in a sense, net protein charge) can modulate the effect. Although our data for the cytochromes *c'* with flavodoxin semiquinone are much more limited than for the cytochromes *c*, in those cases where measurements were possible, ionic strength effects on reaction rate constants were considerably larger for the flavodoxin reactions than for those with FMN. This is also consistent with our previous results.

Quantitative analyses of the transient kinetics of electron transfer in redox proteins are complicated because redox potential differences, steric interactions, and electrostatic effects are all expected to contribute to the observed rate constants. However, we have recently developed methodology for systematically evaluating the separate contributions of these factors for structurally homologous proteins. This involves the use of free flavin semiquinones as reductants, which can be rapidly generated (<1 μs) by laser flash photolysis in the presence of ethylenediaminetetraacetic acid (EDTA), allowing the kinetics of subsequent electron-transfer reactions with redox proteins to be followed spectrophotometrically (Ahmad et al., 1981). In previous work, we have shown that the rate constants for reduction of a large number of homologous cytochromes and high redox potential ferredoxins (HiPIP's) by lumiflavin semiquinone can be correlated with the differences in redox potentials of the reactants (Meyer et al., 1983), as predicted by electron-transfer theory (Marcus, 1964). Furthermore, the intrinsic reactivities toward lumiflavin semiquinone of structurally unrelated proteins having the same type of prosthetic group, after correcting for redox potential, can be related to the relative degree of exposure of the redox centers. For homologous proteins of known structure, it was shown that differences in intrinsic reactivity correlate with steric hindrance to approach of the reductant to the redox center (Meyer et al., 1984).

Electrostatic interactions at the site of electron transfer were quantitated by examining the ionic strength dependence of the kinetics of reduction of a variety of cytochromes and HiPIP's by the negatively charged flavin mononucleotide (FMN) semiquinone (Meyer et al., 1984; Przysiecki et al., 1985). Thus, rate constants at high and low ionic strength were found

† This work was supported by National Institutes of Health Grants AM 15057 (G.T.) and GM 21277 (M.A.C.).

‡ University of Arizona.
§ University of California at San Diego.
‖ Research Institute of Scripps Clinic.

0006-2960/86/0425-1383$01.50/0

to vary by as much as a factor of 5 for some proteins, and both attractive and repulsive interactions were observed. When extrapolated to infinite ionic strength, the FMN rate constants (k_∞) were found to correlate with redox potential differences in the same general manner as for the lumiflavin reactions. The apparent charges at the interaction site for most cytochromes did not correlate with net protein charge, either in sign or in magnitude, but were consistent with more localized interactions. Most recently, we have extended these analyses to protein–protein interactions by studying the reaction of flavodoxin semiquinone with cytochromes and HiPIP's as a function of ionic strength using stopped-flow methods (Tollin et al., 1984; Przysiecki et al., 1985). As was the case with the FMN reactions, we were able to extrapolate rate constants to infinite ionic strength and to show a relationship between k_∞ values and the differences in redox potentials. The sign of the electrostatic interactions was entirely consistent with the results obtained with free FMN. However, the magnitudes of redox potential, steric, and electrostatic effects observed for the flavodoxin reactions were much larger than those for free FMN reactions and thus establish a quantitative basis for understanding protein–protein interaction specificity.

The cytochromes *c'* are a unique group of bacterial high-spin heme proteins, which are relatively unreactive with the usual heme ligands except for carbon monoxide and ethyl isocyanide (Meyer & Kamen, 1982; Rubinow & Kassner, 1984). They can be reversibly oxidized and reduced and presumably function in generalized electron transfer in the cell, although no precise role has yet been established. These proteins are isolated in large quantities from the soluble cell fraction and are usually dimeric. They have a single protoheme covalently bound to cysteine residues as in cytochrome *c* and an adjacent histidine residue serves as the fifth ligand. There is usually no sixth ligand, but there are homologous proteins known as cytochromes *c*-556 that have a methionine sixth ligand (Moore et al., 1982). The heme is bound very near the C-terminus of the peptide chain, which contains approximately 125–130 amino acid residues. The amino acid sequences are known for a relatively large number of species (Ambler et al., 1981), and the three-dimensional (3-D) structure of one example (*Rhodospirillum molischianum*) has been determined (Weber et al., 1981a,b; Finzel et al., 1985). In our previous survey, we found that the cytochromes *c'* were more reactive with lumiflavin semiquinone than were the low-spin cytochromes homologous to mitochondrial cytochrome *c* (Meyer et al., 1983). We ascribed this greater intrinsic reactivity to the much larger exposure of the heme to solvent in these cytochromes. We now report a more extensive characterization of the reactions of the cytochromes *c'*, both with free flavins and with flavodoxin, which both confirm and extend our previous findings.

Materials and Methods

The laser flash photolysis and stopped-flow techniques and the methods of data collection and analysis were as described previously (Ahmad et al., 1981; Simondsen & Tollin, 1983; Meyer et al., 1983, 1984; Tollin et al., 1984; Przysiecki et al., 1985). In all cases, pure proteins were prepared according to the general procedures of Bartsch (1978). The pseudo-first-order decay of the flavin semiquinone and the appearance of the reduced cytochrome were monitored at 620 nm for the high-spin proteins (cytochromes *c'*) and at 585 nm for the low-spin proteins (cytochromes *c*-556 and *c*-554) under anaerobic conditions over 3–4 half-lives. Protein concentrations were varied over a 5–10-fold range, minimally at ~15 μM and maximally at ~150 μM. Typically four to five concentrations were used to determine the second-order rate constants. No saturation effects were observed. FMN was purified by passage through a Bio-Gel P-2 gel filtration column equilibrated with double-distilled water (Nagy et al., 1982) and lyophilized. Solutions were made up just prior to use. Standard buffers contained 40 μM flavin, 10 mM EDTA, and 20 mM sodium phosphate, pH 7.0, for lumiflavin and riboflavin experiments. The 16 mM ionic strength buffer for the FMN experiments contained 1 mM EDTA and 5 mM phosphate; the 60 mM ionic strength buffer contained 5 mM EDTA and 16 mM phosphate. Higher ionic strengths were made up with 10 mM EDTA and 20, 52, 100, and 222 mM phosphate, pH 7.0, giving ionic strengths of 96, 160, 256, and 500 mM, respectively.

Redox potentials were measured spectroelectrochemically. An anaerobic solution of cytochrome was placed in a sealed 4-mL volume cuvette containing platinum and silver–silver chloride electrodes, and the redox potential was varied with a Princeton Applied Research potentiostat. The redox buffer contained 10 mM EDTA, 20 mM potassium phosphate, pH 7.0, and the following redox mediators: 1 mM $FeCl_3$, 1 mM $K_3Fe(CN)_6$, and 1 mM methyl viologen. Absorption spectra were monitored with a Cary 118 spectrophotometer. Both oxidative and reductive titrations were performed, and at least 20 data points were collected at an ambient temperature of about 25 °C. Isosbestic points were observed for all cytochromes studied, and oxidative and reductive titrations were within 5 mV or closer. N values from the Nernst equation were all 1 ± 0.1.

The solvent-accessible molecular surface of *R. molischianum* cytochrome *c'* was calculated by using the program MS (Connolly, 1983) and displayed on computer graphics by using the interactive graphics language GRAMPS (O'Donnell & Olson, 1981) and the molecular modeling program GRANNY (Connolly & Olson, 1985). The molecular surface calculation mathematically rolled a water-sized probe sphere (1.4-Å radius) representing a solvent water molecule over the van der Waals surface of the protein. Molecular surface calculations assigned individual van der Waals radii including implicit hydrogen atoms [adapted from McCammon et al. (1979)] to the atomic coordinates of *R. molischianum* cytochrome *c'* obtained from the Brookhaven Protein Database (Bernstein et al., 1977).

Electrostatic potential calculations for the molecular surface used the approach described previously (Getzoff et al., 1983). Partial charges were assigned to the atomic coordinates by using the updated charges (Weiner et al., 1984) of the AMBER data base (Weiner & Kollman, 1981). This dictionary of Mulliken net atomic charges was developed from ab initio linear combination of atomic orbitals–self-consistent field–molecular orbital (LCAO–SCF–MO) calculations on individual amino acids using the STO-3G basis set (three Gaussian functions per Slater-type orbital). All non-hydrogen atoms and all potentially hydrogen-bonding atoms were included explicitly, while a united-atom representation was used for aliphatic and aromatic hydrogen atoms. The amino acid residues were assumed to be in their predominant state of ionization in aqueous solution at physiological pH. His-122 was considered neutral; the imidazole proton was placed on the N^δ nitrogen because the N^ϵ nitrogen is liganded to the heme iron. The C-terminus was assigned a net charge of −1 and the N-terminus a net charge of +1. No solvent water molecules were included in the calculation. Charges for the ferric heme were modified from those assigned to the ferrous heme of myoglobin by ab initio calculations (David Case, personal communication). The electrostatic potential V at a given point

Table I: Effect of Ionic Strength on Oxidation of FMN and Flavodoxin Semiquinones by Cytochromes *c'*, *c*-556, and *c*-554

	$E_{m,7}$ (mV)	net charge[b]	V_{ii} (kcal/mol)	Z_1[a]	$k_\infty \times 10^{-7}$ (M^{-1} s^{-1})
FMN semiquinone reaction					
(N) *Rps. palustris c*-556	230	0	−1.00	+1.2	3.40
(O) *Rps. sphaeroides c*-554	203	(−10)	+2.41	−2.9	6.96
(A) *Agrobacterium c*-556	180	−2			
(B) *Alcaligenes* sp. *c'*	130	+3	−2.49	+3.0	2.74
(C) *R. salexigens c'*	95	(0)	+2.59	−3.1	6.43
(D) *Rps. palustris c'*	94	+3	−2.43	+2.9	2.02
(E) *Rps. gelatinosa c'*	60	+2	−1.24	+1.5	2.35
(F) *Rps. capsulata c'*	51	−7	+0.84	−1.0	2.72
(G) *R. tenue* 3761 *c'*	45	+2	−2.66	+3.1	1.43
(H) *Rps. sphaeroides c'*	30	−5	0	0	3.40
(P) *E. halophila*[c] *c'*	30	(−20)			
(I) *C. vinosum c'*	18	−5	+1.03	−1.2	4.36
(J) *R. molischianum c'*	14	+1	−1.55	+1.8	1.86
(K) *R. photometricum c'*	14	−1	−1.14	+1.3	2.37
(L) *R. rubrum c'*	3	−1	−0.84	+1.0	2.26
(M) *Rh. purpureus c'*	3	+2	−1.97	+2.3	1.03
					k_∞ (M^{-1} s^{-1})
flavodoxin semiquinone reaction					
Alcaligenes sp. *c'*			−28.9	+6.9	4.1

[a] The apparent charge on the cytochromes at their interaction sites was obtained from $V_{ii} = \alpha Z_1 Z_2 R_{12} \rho^{-2} D_e^{-1}$, where $\alpha = 128.47$, $Z_2 = -1.9$ or -4.0 (FMN or flavodoxin, respectively), $R_{12} = 3.5$ or 13 Å (FMN or flavodoxin, respectively), $\rho = 4.5$ or 7.25 Å (FMN or flavodoxin, respectively), and $D_e = 50$ or 30 (FMN or flavodoxin, respectively); see text for further discussion. [b] Numbers in parentheses indicate charge estimate based on chromatographic properties; otherwise, the net charge is based on amino acid sequence of the monomer with a ferric heme. The sequence indicates N-terminal glutamine pyrrolidone, but we assumed that the N-terminus is unblocked in the native protein. [c] For this protein, the FMN rate constants were too slow to measure (less than 5×10^6 M^{-1} s^{-1}).

r_0, resulting from the partial charges q_i assigned to the atomic positions r_i, is given by the equation:

$$V = \sum_i q_i / D|r_i - r_0|$$

We have used a linearly distance-dependent dielectric model with a dielectric gradient of 1/Å multiplied by the distance between each partial charge and the calculation point ($|r_i - r_0|$) replacing D. The contributions of each partial charge within 20 Å of the calculation point were summed. To correct for dipoles split by the finite cutoff radius, we used the method of neutral spheres (Weiner & Kollman, 1981): a compensatory charge placed at the cutoff radius ensures that the net charge inside the sphere is 0. The electrostatic potential assigned to each molecular surface point was calculated 1.4 Å above that point along a surface normal vector; this calculation (r_0) represents the center of the solvent probe sphere at the position of its closest approach to the molecule. The electrostatic potentials were mapped onto points of the molecular surface by using a five-color code (see Figure 2).

Theoretical curves [cf. Meyer et al. (1983) for discussion] relating second-order rate constants (k) and redox potential differences (ΔE_m) (cf. Figure 1) were constructed by least-squares fits of the data to the Marcus exponential equation[1] (Marcus, 1968) using two adjustable parameters, ν_{ET}, which is the limiting rate constant at infinite redox potential difference and is a measure of intrinsic reactivity, and $\Delta G^*(0)$, which reflects the structural rearrangements that must occur prior to electron transfer. For the data given in Figure 1, we estimate the errors in evaluating these parameters to be as follows: for ν_{ET}, ±20% for lumiflavin and ±25% for riboflavin, and for $\Delta G^*(0)$, ±10% for lumiflavin and ±15% for riboflavin. The curve shown in Figure 1 for FMN is merely an estimate, and the parameter values should only be considered as being approximate.

Theoretical curves [cf. Meyer et al. (1984) and Tollin et al. (1984) for discussion] for the ionic strength dependence of second-order rate constants involving FMN and flavodoxin as reductants (cf. Figures 3 and 4) were constructed from the theory of Watkins (1984). This approach treats the interaction domains of two reacting molecules as parallel plates with radius ρ, a charge of Z_1 and Z_2 separated by a distance R_{12}, with an effective dielectric constant between the plates of D_e. For analysis, eq 1 was used for a least-squares fit to the data points.

$$\ln k(I) = \ln k_\infty - V_{ii}[X(I)] \quad (1)$$

In this equation, k_∞ is the rate constant extrapolated to infinite ionic strength where all electrostatic factors are screened out, V_{ii} is the electrostatic interaction energy, and $X(I)$ [$X(I) = (1 + \kappa\rho)^{-1} \exp(-\kappa\rho)$, where $\kappa = 0.3295 I^{1/2}$] is an ionic strength dependent term. V_{ii} ($V_{ii} = \alpha Z_1 Z_2 R_{12} D_e^{-1} \rho^{-2}$, where $\alpha = 128.47$ and the other parameters are defined as described above) was evaluated applying eq 1 for a particular value of ρ. Typically, a series of fits at different ρ values were obtained, and the value (±0.5 Å) that yielded the minimum least-squares error was used. Of the parameters that define V_{ii}, all but Z_1 are fixed (see below), allowing a determination of the effective interaction site charge of one of the reactants (cf. Table I and below). Thus, Z_1 (but not the fits to yield V_{ii} and k_∞) is directly proportional to D_e and ρ^2 and inversely proportional to R_{12} and Z_2.

Results and Discussion

In a previous study (Meyer et al., 1983), we showed that the rate constants for reduction of *c*-type cytochromes by lumiflavin semiquinone could be related to differences in redox potential. In addition, a few examples of cytochromes *c'* were found to be intrinsically more reactive with lumiflavin semiquinone than were the *c*-type cytochromes at the same redox potential. We have now examined 13 different species of cytochrome *c'*, as well as 3 low-spin proteins known as cytochromes *c*-556 and *c*-554. There is no sequence available for cytochrome *c*-554, but it has visible spectra and redox potentials analogous to cytochrome *c*-556. Although the range of redox potentials available to us (3–230 mV; see Table I) is not as large as for the *c*-type cytochromes used in the previous study (28–470 mV), it is clear that an analogous relationship exists between the rate constants for reduction of

[1] $\ln k = \ln \nu_{ET} + (1/RT)\{nF\Delta E_m - \Delta G^*(0)/0.693 \ln [1 + \exp[-0.693 nF\Delta E_m/\Delta G^*(0)]]\}$, where F is the Faraday constant and n is the number of electrons.

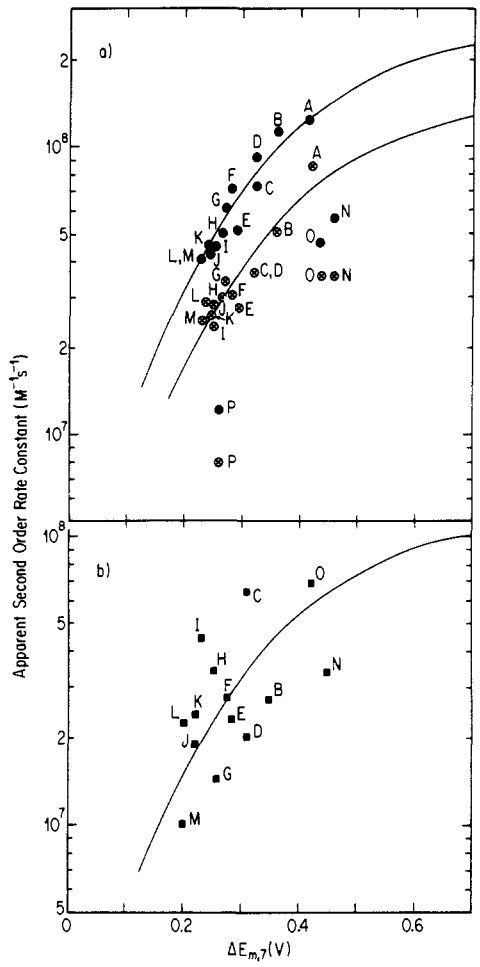

FIGURE 1: Semilog plot of apparent second-order rate constants vs. difference in redox potential between reactants at pH 7 ($\Delta E_{m,7}$). Solid lines are theoretical curves (see Materials and Methods) based on the Marcus exponential equation [cf. Meyer et al. (1983)] with parameters as given below. The parameters were obtained by least-squares fits to the data points (see text for estimates of errors). (a) (●) Lumiflavin, ν_{ET} = 2.8 × 10^8 M^{-1} s^{-1} and $\Delta G^*(0)$ = 3.0 kcal/mol; (⊗) riboflavin, ν_{ET} = 1.5 × 10^8 M^{-1} s^{-1} and $\Delta G^*(0)$ = 3.0 kcal/mol. (b) (■) FMN (rate constants extrapolated to infinite ionic strength), ν_{ET} = 1.2 × 10^8 M^{-1} s^{-1} and $\Delta G^*(0)$ = 3 kcal/mol; these parameters are only approximate (see text). Identification of proteins based on letter designations is given in Table I.

cytochromes *c'* by lumiflavin semiquinone and the differences in redox potential between the reactants (Figure 1a). The more comprehensive study reported here confirms our previous conclusion that this group of electron-transfer proteins (with three exceptions; see below) is approximately 3 times as reactive with lumiflavin semiquinone as are the *c*-type cytochromes of the previous study (ν_{ET} values are 2.8 × 10^8 and 1 × 10^8 M^{-1} s^{-1}, respectively). This increase in reactivity is consistent with the fact that the heme is more exposed in the cytochromes *c'*, at least in the one case for which structural information is available. Thus, in tuna cytochrome *c*, the edge of one pyrrole and the thioether bridge are exposed to solvent, whereas in *R. molischianum* cytochrome *c'*, half of the heme face and the histidine fifth ligand are exposed (Figure 2). The question of steric accessibility is more complex than this, however, inasmuch as in the *c'* cytochrome the heme is located at the bottom of a deep groove in the surface of the protein, which is about 10–15 Å deep and equally as wide (Figure 2). Although lumiflavin is small enough to enter this groove, larger molecules (such as other proteins) might not be able to effectively penetrate to the heme surface (see below). Furthermore, the movement of lumiflavin within the groove is likely to be more restricted than at a smoother surface such as is present in the cytochromes *c*.

The rate constants for reaction between lumiflavin semiquinone and three of the cytochromes, *Rhodopseudomonas palustris c*-556, *Rhodopseudomonas sphaeroides c*-554, and *Ectothiorhodopspira halophila c'* (N, O, and P, respectively, in Figure 1a), are anomalously low and appear to fit a separate, but approximately parallel, theoretical curve (not shown). We can therefore predict that these three proteins will be found to have structural differences that result in more restricted access to the heme than in the general *c'* class.

Two of the three proteins that are less reactive have low-spin iron (and have a methionine sixth ligand), although *Agrobacterium c*-556, which is also low spin, has normal reactivity. Given that structural homology exists in the cytochrome *c'* family, on the basis of amino acid sequence homology, spin state does not appear to have a significant effect on reduction kinetics. However, a definitive conclusion on this point will have to await further data. *Rps. palustris c'* and *Rps. palustris c*-556 are the only clearly monomeric proteins in the group; the former has normal reactivity and the latter is less reactive than the average. On the basis of the 3-D structure of *R. molischianum c'*, which shows that the groove containing the heme is made up of contributions from both peptide chains of the dimer, we might expect the monomeric proteins to be more reactive than the dimers because of an opening up of the region surrounding the heme. This is clearly not the case and provides further evidence that there are differences in the 3-D structures of the various members of the cytochrome *c'* family. Additional structural work is required in order to clarify this situation.

The rate constants for reduction of the cytochromes *c'* by riboflavin semiquinone can also be related to redox potential differences as shown in Figure 1a. The rate constants for these reactions average approximately 54% of those for the lumiflavin semiquinone reactions (ν_{ET} = 1.5 × 10^8 M^{-1} s^{-1}). This is a somewhat larger decrease than was previously found (Meyer et al., 1984) for the cytochromes homologous to mitochondrial cytochrome *c* (which averaged 70% of the lumiflavin values) and may be due to a greater degree of steric hindrance in the case of a reaction that occurs at a concave as opposed to a convex protein surface. The riboflavin results with the *Rps. palustris*, the *Rps. spheroides*, and the *E. halophila* cytochromes are consistent with the lower reactivity of these proteins toward lumiflavin (Figure 1a).

The rate constants for reduction of the cytochromes *c'* by the negatively charged FMN semiquinone were ionic strength dependent as is shown in Figure 3. Both attractive and repulsive interactions were observed. Identical results were obtained (with *R. molischianum c'*) whether potassium phosphate or potassium chloride was used to adjust ionic strength, indicating that the results were not due to a specific anion effect. Theoretical curves (Figure 3) based on the Watkins (1984) model of electrostatic interactions in proteins were computed, and rate constants were extrapolated to infinite ionic strength (Table I). The FMN semiquinone–cytochrome *c'* rate constants at infinite ionic strength (k_∞) can also be related to redox potential differences, as was done for the lumiflavin and riboflavin reactions (Figure 1b). There is clearly a greater degree of scatter in the data points than for the other flavin homologues, as was also the case with FMN in our previous studies (Meyer et al., 1984; Przysiecki et al., 1985), and it is therefore not possible to fit these data to a unique theoretical curve. Some of the discrepancies may be due to differences in the shape of the groove on the surface

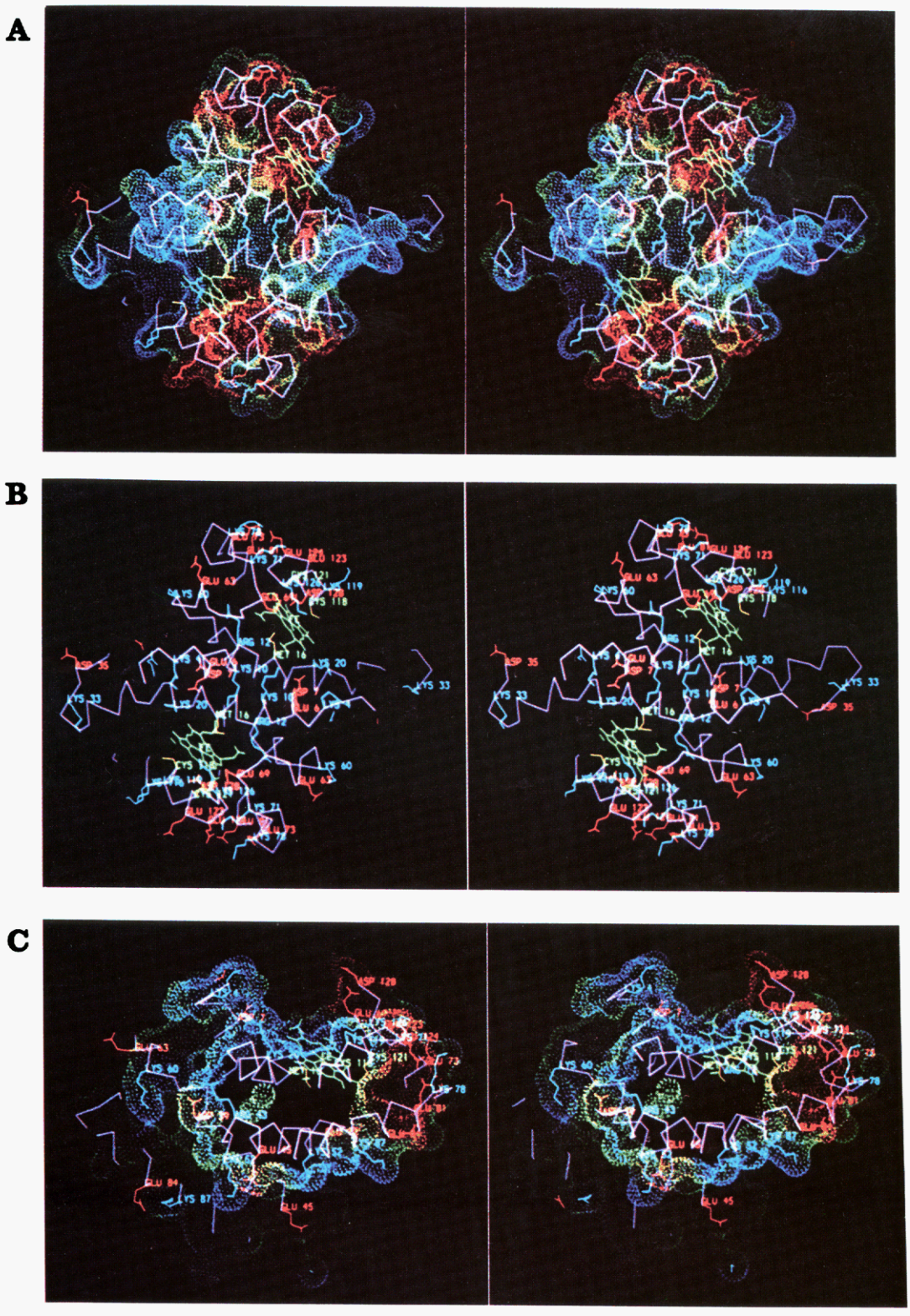

FIGURE 2: Stereoviews of *R. molischianum* cytochrome *c'*. (A) Electrostatic surface of the dimer, distant-dependent dielectric model, where the dielectric constant is equal to the distance in angstroms between the point charge and the calculation point. The color code for the electrostatic potential is as follows: red, >−21 kcal/mol; yellow, <−21 > −7 kcal/mol; green, <+7 > −7 kcal/mol; cyan, >+7 < +21 kcal/mol; blue, >+21 kcal/mol. Note the groove that runs diagonally from upper right to lower left. (B) Partial backbone and side-chain view to illustrate positions of the charged side chains (same view as panel A). (C) A cutaway view of the cytochrome *c'* dimer to illustrate the charge asymmetry of the heme pocket and another view of the groove (at the top).

of cytochrome *c'*, which result in changes in the types of interactions that can occur with the various flavin analogues. Support for this idea may be obtained by a detailed comparison of the lumiflavin, riboflavin, and FMN results. Thus, *Rps. spheroides* c-554, *Rhodospirillum salexigens c'*, and *Chromatium vinosum c'* have anomalously high rate constants for FMN (Table I), suggesting that the phosphate group of FMN may provide a favorable interaction, whereas *Alcaligenes c'*, *Rps. palustris c'*, *Rhodospirillum tenue c'*, and *Rhodocyclus purpureus c'* show a greater than average separation of the three rate constants. This suggests that there are topographical differences among the cytochromes *c'*, which presumably

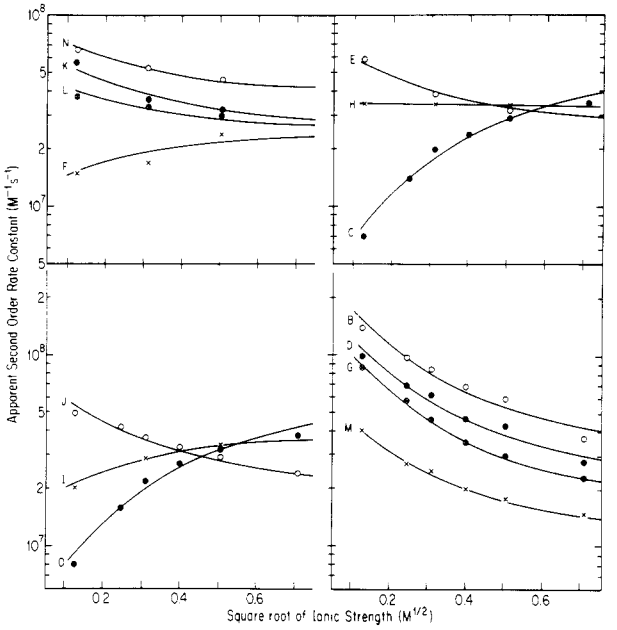

FIGURE 3: Semilog plots of apparent second-order rate constants for reduction of cytochromes *c'* by FMN semiquinone vs. square root of ionic strength. Curves are lettered as in Figure 1. Solid lines are theoretical curves based on the Watkins (1984) model (see text for details).

would be detected by X-ray structure determination.

Table I also presents the apparent charges (Z_1) at the site of interaction between the various cytochromes *c'* and FMN semiquinone. These were calculated from V_{ii}, which is obtained from a least-squares fit to the ionic strength profile. D_e was taken as 50 for the FMN semiquinone reactions; this value reflects the expected surface dielectric (Rees, 1980) and is consistent with our previous studies with *c*-type cytochromes and HiPIP's (Meyer et al., 1984; Przysiecki et al., 1985). ρ was taken as 4.5 Å; this value gave the best fits to the data and is also consistent with our previous studies (Meyer et al., 1984). R_{12} was set equal to 3.5 Å, the sum of van der Waals radii.

Neither the signs nor the magnitudes of the ionic strength effects correlate with net protein charge (Table I). Thus, *Rhodospirillum rubrum* and *Rhodospirillum photometricum* cytochromes *c'* have a small net negative protein charge, but the reactions with FMN semiquinone show a small positive charge at the interaction site. *Rps. spheroides c'* has a larger net negative protein charge but has almost no ionic strength effect with FMN semiquinone. *Rps. palustris c*-556 is a neutral protein, but it shows a significant positive charge at the site of interaction with FMN semiquinone. For the *R. molischianum* and *R. tenue* cytochromes, the calculated charge at the electron-transfer site is larger in magnitude than the net protein charge. These results are similar to those obtained with *c*-type cytochromes related to mitochondrial cytochrome *c* and, to a lesser extent, with the HiPIP's (Meyer et al., 1984; Przysiecki et al., 1985). With these latter proteins, local interactions at the site of electron transfer appeared to dominate in most cases, but where there was very little charge at the localized site of electron transfer, then more distant charges exerted a weak effect. In cytochrome *c'* a number of charged residues are located near the heme, but unlike mitochondrial cytochrome *c* in which these side chains are all basic, there is a complicated mixture of positive and negative residues. Computer graphics representations of the calculated electrostatic potential at the surface of *R. molischianum c'* are shown in parts A and C of Figure 2. The kinetic results with FMN indicate that there is a positive charge at the site of interaction, and this can be identified with contributions from Lys-20, Lys-33, Lys-119, Lys-126, and the N-terminus and Lys-4 of the adjacent subunit in the dimer. Negative charges at the C-terminus probably modulate the effect. Basic residues are conserved at positions 119 and 126 in all cytochromes *c'*, but the other residues that contribute to the electrostatic field near the heme are highly variable, and insertions and deletions complicate the analyses. In most cases, one would not be able to predict the sign of the interaction between charged reactants with any degree of confidence. For example, both *C. vinosum* and *Rhodopseudomonas capsulata* cytochromes *c'* show a negative charge at the site of electron transfer. For *Chromatium c'*, Lys-20 is substituted by Gly, Lys-33 is deleted (*R. molischianum c'* numbering), and there are additional negative charges at positions 31 and 34. Furthermore, the N-terminal 10 residues are more acidic overall, and Lys-4 is replaced by Ser. However, Glu-69 and Asp-128 are replaced by Lys, and the C-terminal region is more positively charged. The net effect of these changes should be an increased negative charge in the vicinity of the heme. Thus, this protein shows the clearest correlation between amino acid substitutions and observed ionic strength effects. In *Rps. capsulata c'*, it is less obvious why the ionic strength effects are reversed. Lys-20 is replaced by Gly, but Lys-24 should be functionally equivalent. Lys-33 is deleted, but there is a nearby Lys-31. The sign change apparently results from the replacement of Lys-4 by Asp (*R. molischianum c'* numbering) and a more acidic C-terminal region. In both cases 3-D structures and electrostatic potential calculations are needed to fully analyze the observed electrostatics. This example is typical of the cytochromes *c'* as a whole and underscores the need for additional structure determinations. We have already seen from steric effects on kinetics that there are likely to be substantial variations in 3-D structures among these proteins.

Many of the cytochromes *c'* have redox potentials that are too low to allow electron transfer with flavodoxin semiquinone to occur on a time scale that is easily accessible to stopped-flow methods. However, several proteins, which showed a positive charge at the site of interaction with FMN semiquinone, were found to react at a measurable (albeit slow) rate with flavodoxin semiquinone. These reactions had an ionic strength dependence with the same sign as was found for the corresponding FMN reactions (Figure 4). As was done for the FMN system, the apparent charge at the interaction domain (Z_1) was calculated for the reaction of flavodoxin semiquinone and *Alcaligenes* cytochrome *c'* (Table I). The calculated value (+6.9) is significantly larger than that observed with FMN semiquinone, consistent with the larger interaction domain expected for protein–protein interactions. For the calculation, ρ was taken as 7.25 Å, a value identical with that used for the flavodoxin–cytochrome *c* system (Tollin et al., 1984), D_e was set equal to 30 to allow for some exclusion of water on transient complex formation (this is the same value used previously for the HiPIP's), R_{12} was taken as 13 Å (see below), and Z_2 was set at −4 (Tollin et al., 1984). Upon extrapolation to infinite ionic strength, the k_∞ for *Alcaligenes* cytochrome *c'* was 4 M^{-1} s^{-1} (see Table I). A k_∞ value of ~ 1 M^{-1} s^{-1} for *Rps. palustris* and *R. molischianum* cytochromes *c'* can be estimated from the data given in Figure 4. These rate constants are 3 orders of magnitude smaller than those obtained for reactions between flavodoxin semiquinone and those cytochromes related to mitochondrial cytochrome *c* that have approximately the same redox potential (Tollin et al., 1984). Thus, *Chlorobium* cytochrome *c*-555 ($E_{m,7}$ = 150 mV) has a k_∞ value with flavo-

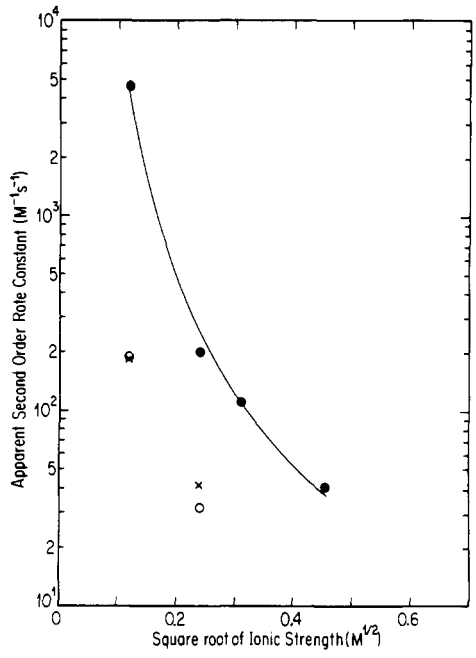

FIGURE 4: Semilog plots of apparent second-order rate constants for reduction of cytochromes *c'* by flavodoxin semiquinone vs. square root of ionic strength. The solid line is the theoretical curve as in Figure 3 (see text). Symbols: (●) *Alcaligenes* sp. *c'*; (○) *Rps. palustris c'*; (×) *R. molischianum c'*.

doxin semiquinone of 3×10^3 M^{-1} s^{-1}, and *E. halophila c*-551 ($E_{m,7}$ = 58 mV) has a k_∞ value of 2×10^3 M^{-1} s^{-1}. *Rps. palustris c'* appears to be less reactive with flavodoxin semiquinone than might be expected on the basis of its redox potential and the relative reactivities of *Alcaligenes c'* and *R. molischianum c'*. Again this is an example of reactivity that is inconsistent with expectation on the basis of the 3-D structure of *R. molischianum c'*.

As stated above, lumiflavin is intrinsically more reactive with cytochrome *c'* than with mitochondrial cytochrome *c* because of a greater extent of heme exposure in the former than in the latter. However, the heme in the *c'* cytochromes is located at the bottom of a deep groove (cf. Figure 2), which would prevent flavodoxin from approaching closer than about 10–15 Å without structural rearrangements and which, because of the exponential dependence of rate constant on distance (Miller et al., 1984), could account for the anomalously slow reaction. With computer-generated graphics, a sphere 15 Å in radius was brought up to the heme crevice of *R. molischianum* cytochrome *c'* (to approximate the approach of flavodoxin). In this case, close approach to the heme was blocked. However, rotation of Asp-128, Lys-4, Lys-20, Lys-33, Lys-126, and the N-terminus about single bonds allowed approach of the sphere to the van der Waals surface of the NDI nitrogen of His-122 (the ligated histidine). Other approaches to the heme plane yielded generally similar results. Thus, the substantial decrease in the rate of reduction by flavodoxin could result from a *dynamic* steric hindrance, due to the requirement for the appropriate groups to rotate out of the way in order for a productive collision to occur. Although not mentioned in the crystallographic analysis of *R. molischianum* cytochrome *c'* (Weber et al., 1981a,b; Finzel et al., 1985), this groove appears to be important for the electron-transfer mechanism of the protein. Thus, unless another electron-transfer protein has a structure that is complementary to the groove containing the heme, one would expect it to react much more slowly with the *c'* cytochromes than would be predicted on the basis of redox potentials alone. This is an especially clear demonstration of the use of surface topography as a dominant factor in controlling reaction rate.

Although our data are necessarily limited, it is clear that, at least for the three cytochromes *c'* shown in Figure 4, the effects of ionic strength on reaction rate constants are considerably larger for the flavodoxin system than for FMN. This is consistent with our previous studies (Tollin et al., 1984; Przysiecki et al., 1985) and provides further support for our contention that electrostatic interactions, as well as steric effects, between the electron-transfer domains of redox proteins can provide an appreciable level of kinetic discrimination and thus play an important role in the establishment of biological specificity.

Supplementary Material Available

Three tables giving the rate constants used in Figures 1a, 3, and 4 (3 pages). Ordering information is given on any current masthead page.

Registry No. *c*-556, 37306-15-3; *c*-554, 52932-67-9; *c'*, 9035-41-0; FMN semiquinone, 34469-63-1; riboflavin semiquinone, 35919-91-6; lumiflavin semiquinone, 34533-61-4.

References

Ahmed, I., Cusanovich, M. A., & Tollin, G. (1981) *Proc. Natl. Acad. Sci. U.S.A. 78*, 6724–6728.

Ambler, R. P., Bartsch, R. G., Daniel, M., Kamen, M. D., McLellan, L., Meyer, T. E., & Van Beeuman, J. (1981) *Proc. Natl. Acad. Sci. U.S.A. 78*, 6854–6857.

Bartsch, R. G. (1978) in *The Photosynthetic Bacteria* (Clayton, R. K., & Sistrom, W. R., Eds.) Chapter 13, pp 249–279, Plenum Press, New York.

Bernstein, F. C., Koetzle, T. F., Williams, G. J. B., Meyer, E. F., Brice, M. D., Rogers, J. R., Kennard, O., Shimanouchi, T., & Tasumi, M. (1977) *J. Mol. Biol. 112*, 535–542.

Connolly, M. L. (1983) *Science (Washington, D.C.) 221*, 709–713.

Connolly, M. L., & Olson, A. J. (1985) *Comput. Chem. 9*, 1–6.

Finzel, B. C., Weber, P. C., Hardman, K. D., & Salemme, F. R. (1985) *J. Mol. Biol. 186*, 627–643.

Getzoff, E. D., Tainer, J. A., Weiner, P. K., Kollman, P. A., Richardson, J. S., & Richardson, D. C. (1983) *Nature (London) 306*, 287–288.

Marcus, R. A. (1964) *Annu. Rev. Phys. Chem. 15*, 155–196.

Marcus, R. A. (1968) *J. Phys. Chem. 72*, 891–899.

McCammon, J. A., Wolynes, P. G., & Karplus, M. (1979) *Biochemistry 18*, 927–942.

Meyer, T. E., & Kamen, M. D. (1982) *Adv. Protein Chem. 35*, 105–212.

Meyer, T. E., Przysiecki, C. T., Watkins, J. A., Bhattacharyya, A., Simondsen, R. P., Cusanovich, M. A., & Tollin, G. (1983) *Proc. Natl. Acad. Sci. U.S.A. 80*, 6740–6744.

Meyer, T. E., Watkins, J. A., Przysiecki, C. T., Tollin, G., & Cusanovich, M. A. (1984) *Biochemistry 23*, 4761–4767.

Miller, J. R., Beitz, J. V., & Huddleston, R. K. (1984) *J. Am. Chem. Soc. 106*, 5057–5068.

Moore, G. R., McClune, G. J., Clayden, N. J., Williams, R. J. P., Alsaadi, B. M., Bartsch, R. G., Meyer, T. E., & Kamen, M. D. (1982) *Eur. J. Biochem. 123*, 73–80.

Nagy, J., Knoll, J., Kenney, W. C., & Singer, T. P. (1982) in *Flavins and Flavoproteins* (Massey, V., & Williams, C. H., Jr., Eds.) pp 573–578, Elsevier/North-Holland, New York.

O'Donnell, T. J., & Olson, A. J. (1981) *Comput. Graphics 15*, 133.

Przysiecki, C. T., Cheddar, G., Meyer, T. E., Tollin, G., & Cusanovich, M. A. (1985) *Biochemistry 24*, 5647–5652.
Rees, D. C. (1980) *J. Mol. Biol. 141*, 323–326.
Rubinow, S. C., & Kassner, R. J. (1984) *Biochemistry 23*, 2590–2595.
Simondsen, R. P., & Tollin, G. (1983) *Biochemistry 22*, 3008–3016.
Tollin, G., Cheddar, G., Watkins, J. A., Meyer, T. E., & Cusanovich, M. A. (1984) *Biochemistry 23*, 6345–6349.
Watkins, J. A. (1984) Ph.D. Thesis, University of Arizona, Tucson, AZ.
Weber, P. C., Bartsch, R. G., Cusanovich, M. A., Hamlin, R. C., Howard, A., Jordan, S. R., Kamen, M. D., Meyer, T. E., Weatherford, D. W., Xuong, N. H., & Salemme, F. R. (1981a) *Nature (London) 286*, 302–304.
Weber, P. C., Howard, A., Xuong, N. H., & Salemme, F. R. (1981b) *J. Mol. Biol. 153*, 399–424.
Weiner, P. K., & Kollman, P. A. (1981) *J. Comput. Chem. 2*, 287–303.
Weiner, S. J., Kollman, P. A., Case, D. A., Singh, U. C., Ghio, C., Alagona, G., Profeta, S., Jr., & Weiner, P. (1984) *J. Am. Chem. Soc. 106*, 765–784.

Thermodynamic Properties of Oxidation–Reduction Reactions of Bacterial, Microsomal, and Mitochondrial Cytochromes P-450: An Entropy–Enthalpy Compensation Effect†

Yung-Yuan Huang,‡,§ Takayuki Hara,‡ Stephan Sligar,∥ Minor J. Coon,⊥ and Tokuji Kimura*,‡

Department of Chemistry, Wayne State University, Detroit, Michigan 48202, Department of Biochemistry, University of Illinois, Urbana, Illinois 61801, and Department of Biological Chemistry, University of Michigan, Ann Arbor, Michigan 48109

Received May 21, 1985; Revised Manuscript Received October 24, 1985

ABSTRACT: An optically transparent thin-layer electrode cell with a very small volume was used for determination of the formal reduction potentials of bacterial, microsomal, and mitochondrial cytochromes P-450. At an extrapolated zero concentration of dye, the bacterial cytochrome from *Pseudomonas putida* catalyzing the hydroxylation of camphor and the adrenal mitochondrial cytochrome catalyzing the cholesterol side-chain cleavage reaction had formal reduction potentials of −168 and −285 mV (pH 7.5 and 25 °C), respectively. The oxidation–reduction potentials for the rabbit liver microsomal cytochrome P-450 induced by 3-methylcholanthrene and the mitochondrial cytochrome for steroid 11β-hydroxylation were found as −360 and −286 mV, respectively. Potential measurements at different temperatures allowed documentation of the standard thermodynamic parameters for cytochrome P-450 reduction for the first time. All cytochromes tested were found to have a relatively large negative entropy change upon reduction. The extent of these changes is comparable to that observed for the ferric–ferrous couple of cytochrome *c*. An entropy–enthalpy compensation effect was observed among the four cytochromes P-450 examined although the correlation is weaker than that observed with cytochrome *c* isolated from various sources.

Cytochrome P-450[1] is distributed widely in the biosphere, being found in mammals, plants, insects, bacteria, and yeast, and serves as a terminal oxidase of a variety of monooxygenase reactions (White & Coon, 1980). The various cytochromes P-450 display considerable homology at both the amino acid and nucleotide primary sequence levels (Morohashi et al., 1984). In order to investigate the possible functional similarities among bacterial, microsomal, and mitochondrial cytochromes in light of their common features of electron-transfer reactions resulting in the ferric–ferrous reduction of the heme iron, we have measured their formal oxidation–reduction potentials at different temperatures, thus determining the standard thermodynamic parameters for this redox couple. Clearly observed is an entropy–enthalpy compensation effect among the various cytochromes P-450 tested.

Materials and Methods

Materials. BV and IC were obtained from K and K Corp. BV was recrystallized twice from cold methanol by the addition of ether. IC was recrystallized twice from water by the addition of 2-propanol. Glucose oxidase (type VII) and catalase thymol free) were purchased from Sigma.

Methods. P-450$_{scc}$ and P-450$_{11\beta}$ were prepared from bovine adrenal cortex mitochondria. Purification of P-450$_{scc}$ was performed by the method described previously (Hsu, 1984). The specific content of final preparations was about 8

† This study was supported by grants from the National Institutes of Health (AM-12713 to T.K., GM-31756 to S.S., and AM-10339 to M.J.C.).

* Address correspondence to this author.
‡ Wayne State University.
§ Present address: American Hospital Supply, Irvine, CA 92715.
∥ University of Illinois.
⊥ University of Michigan.

[1] Abbreviations: BV, benzylviologen; DOC, deoxycorticosterone; DTT, dithiothreitol; $E^{\circ\prime}$, formal reduction potential vs. normal hydrogen electrode; EDTA, ethylenediaminetetraacetate; IC, indigo carmine; *n*, the electron equivalent per reaction; NHE, normal hydrogen electrode; SCE, saturated calomel electrode; P-450, cytochrome P-450; P-450$_{cam}$, cytochrome P-450 catalyzing camphor 5-exo-hydroxylation; P-450$_{LM_4}$, cytochrome P-450 induced by 3-methylcholanthrene or β-naphthoflavone and purified from liver microsomes of rabbits; P-450$_{11\beta}$, cytochrome P-450 catalyzing steroid 11β-hydroxylation; P-450$_{scc}$, cytochrome P-450 catalyzing cholesterol side-chain cleavage reaction; *r*, correlation coefficient.

0006-2960/86/0425-1390$01.50/0